



Contents lists available at ScienceDirect

Bioorganic & Medicinal Chemistry

journal homepage: www.elsevier.com/locate/bmc

Discovery of 3-acetyl-4-hydroxy-2-pyranone derivatives and their difluoridoborate complexes as a novel class of HIV-1 integrase Inhibitors

Kavya Ramkumar^a, Konstantin V. Tambov^b, Rambabu Gundla^a, Alexandr V. Manaev^b, Vladimir Yarovenko^b, Valery F. Traven^b, Nouri Neamati^{a,*}

^a Department of Pharmacology & Pharmaceutical Sciences, University of Southern California, School of Pharmacy, Room 304, 1985 Zonal Avenue, Los Angeles, CA 90089, USA

^b D. Mendeleev University of Chemical Technology of Russia, Miusskaja st.3, Moscow 125047, Russia

ARTICLE INFO

Article history:

Received 30 May 2008

Revised 15 August 2008

Accepted 20 August 2008

Available online 30 August 2008

Keywords:

HIV integrase inhibitor

Boron

Pyranone

Docking

GOLD

eHITS

ABSTRACT

HIV-1 integrase (IN) has emerged as an important therapeutic target for anti-HIV drug development. Its uniqueness to the virus and its critical role in the viral life cycle makes IN suitable for selective inhibition. The recent approval of Raltegravir (MK-0518) has created a surge in interest and great optimism in the field. In our ongoing IN drug design research, we herein report the discovery of substituted analogs of 3-acetyl-4-hydroxy-2-pyranones and their difluoridoborate complexes as novel IN inhibitors. In many of these compounds, complexation with boron difluoride increased the potency and selectivity of IN inhibition. Compound **9** was most active with an IC₅₀ value of 9 μM and 3 μM for 3'-processing and strand transfer inhibition, respectively.

© 2008 Elsevier Ltd. All rights reserved.

1. Introduction

In recent years, HIV-1 integrase (IN) has emerged as an important therapeutic target for the design of anti-HIV agents. IN catalyzes the insertion of HIV proviral DNA into the host genome. This integration occurs via a multi-step process, in which the cleavage of a dinucleotide pair from the 3'-end of the proviral DNA (3'-processing) and the subsequent insertion of the shortened strand into the host genome (strand transfer) are the key catalytic functions of the enzyme.¹ Compounds inhibiting IN block one or both of these steps. There is a plethora of literature describing diverse structural classes of IN inhibitors.^{2–4} Among these, the β-diketo acid class of compounds has shown selective IN inhibition and considerable clinical efficacy. Previous studies from our lab have also identified several potent and selective IN inhibitors based on β-diketo acid and chalcone pharmacophores.^{5,6} Several other pharmacophore based approaches have also resulted in diverse IN inhibitors.^{7,8} Many of these compounds have been reported to significantly suppress retroviral replication.^{9,10} Raltegravir (MK-0518), a pyrimidone carboxamide, was recently approved by the FDA as an anti-HIV drug and is the first member of the new class of IN inhibitor drugs.¹¹ Elvitegravir (GS-9137), another IN inhibitor based on a dihydroquinoline carboxylic acid structure, is undergoing advanced clinical evaluations.^{12,13} However, the propensity for

emergence of resistant IN strains necessitates continual efforts to design structurally novel IN inhibitors.^{3,14} Moreover, studies with diverse classes of inhibitors may also help better understand the mechanisms of IN action.

In our on-going efforts to identify structurally diverse compounds with IN inhibitory activity, we discovered a novel class of substituted analogs of 3-acetyl-4-hydroxy-pyranone and their difluoridoborate complexes that show potent IN inhibitory effect. Various substituted pyranones have been previously reported to exhibit anticancer, antimicrobial, anticoagulant and HIV protease inhibitory properties.^{15,16} Similarly, boron-containing compounds have been used in boron capture therapy for cancer treatment and as metallocarboranes for HIV protease inhibition.^{17,18} This is however the first report of substituted pyranones and their difluoridoborate complexes exhibiting potent IN inhibitory activities. We herein report the synthesis and IN inhibition profile of these novel compounds as well as the results of molecular docking studies, exploring the binding interactions of potent compounds in the IN active site.

2. Results and discussion

2.1. Chemistry

Recently, we have found complexation with boron to greatly increase the reactivity of acetyl(hydroxy)hetarenes toward

* Corresponding author. Tel.: +1 323 442 2341; fax: 1 323 442 1390.
E-mail address: neamati@usc.edu (N. Neamati).

aldehydes. We prepared various α,β -unsaturated ketones from the reaction between 3-acetyl-4-hydroxycoumarin difluoridoborate complex and carbonyl derivatives.^{19–21} These products have high electronic absorption and emission. Difluoridoborate complexes of 2-quinoline and 2-pyranone derivatives of coumarins also possessed high reactivity toward aldehydes. This led to easy derivatization of the 3-acetyl-function in acetylhydroxyhetarenes. The starting compound 3-acetyl-6-methyl-2-oxo-2H-pyran-4-yl difluoridoborate (**1**) was prepared, using the method previously described for coumarin analogs.¹⁹

Condensation of 3-acetyl-6-methyl-2-oxo-2H-pyran-4-yl difluoridoborate **1** with triethyl orthoformate in acetic anhydride in the presence of triethylamine formed symmetric B-complex **1** (Scheme 1). Condensation of 3-acetyl-6-methyl-2-oxo-2H-pyran-4-yl difluoridoborate complex **1** with *p*-R-substituted benzaldehydes provided complexes **2**, **3** and **5** by heating of the starting compounds in Ac₂O or AcOH–H₂SO₄ mixture (Scheme 2). Compounds **4** and **6** have been prepared by the hydrolysis of **2**, **3** and **5** in EtOH–H₂O in the presence of Na₂CO₃. Condensation of **1** with heterocyclic aldehydes in similar conditions provided complexes **7**, **9** and **11**. Compounds **8**, **10** and **12** were prepared by subsequent hydrolysis (Scheme 3) of these complexes.

Complexes **13** and **15** were obtained from the condensation of 3-acetyl-6-methyl-2-oxo-2H-pyran-4-yl difluoridoborate **1** with *p*-R-substituted aldehydes. Hydrolysis of **13** and **15** resulted in unsaturated aldehydes **14** and **16** (Scheme 4). Due to the complexation of 3-acetyl-4-hydroxy-6-methyl-2-pyranone with BF₃, the 6-methyl group was reactive toward aldehydes as well. Condensation of complexes **2**, **3** and **5** with *p*-Me₂N-benzaldehyde resulted in complexes **17**, **19** and **21**. Subsequent hydrolysis gave compound **18**, **20** and **22** in good yields (Scheme 5). Structures of all compounds have been confirmed by ¹H NMR and mass spectra, as well as by elemental analysis.

2.2. In vitro IN inhibitory profile of novel compounds

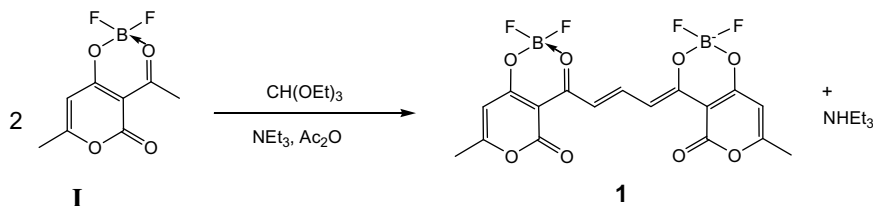
Inhibition of the IN catalytic activities were measured using an in vitro assay specific for IN. Table 1 presents the structure of each compound and its IC₅₀ values for IN inhibition. Compound **1**, which has a dimeric 3-acetyl-4-hydroxy-6-methyl-pyranone structure and is complexed with boron difluoride, inhibited 3'-processing and strand transfer activities of IN with IC₅₀ values of 13 ± 8 and 7 ± 2 μM, respectively. These results led us to further study some key structural features by modifying compound **1**.

Compound **2**, in which boron is complexed with the pyranone structure containing *N,N*-dimethylaniline, showed moderate selectivity towards strand transfer inhibition (IC₅₀ value of 56 ± 1 μM). Compounds **3** and **4** share a bromobenzene substitution at the 3-acetyl position in the pyranone structure. While compound **4** lacked any IN inhibition at 100 μM, its boron complexed analog, compound **3**, exhibited potent inhibition of 3'-processing (IC₅₀ value of 12 ± 6 μM) and a 3-fold selectivity against strand transfer (IC₅₀ of 4 ± 2 μM). Compounds **5** and **6**, with a fluorobenzene substitution showed similar activity profile to compounds **3** and **4**. Compound **5** inhibited 3'-processing with an IC₅₀ of 9 ± 3 μM and strand transfer with an IC₅₀ of 16 ± 4 μM. Compound **6** showed a moderate inhibition of 3'-processing (IC₅₀ value of 64 μM) but did not inhibit strand transfer at 100 μM.

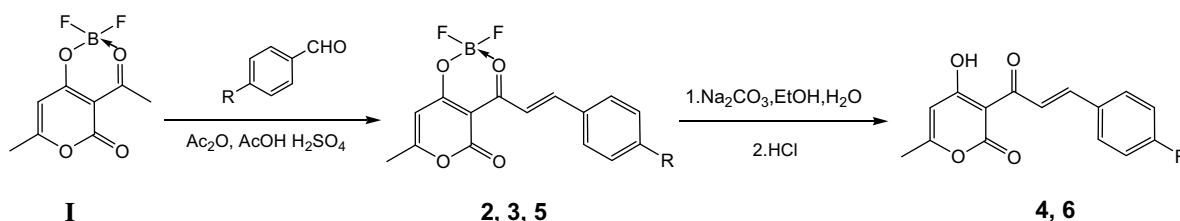
Compound **8** with *N,N*-dimethylthiophen-2-amine substitution inhibited 3'-processing and strand transfer with IC₅₀ values of 19 and 11 μM, respectively. However, its boron complexed derivative, compound **7**, did not possess any IN inhibitory effect. Compounds **9** and **10** showed a 3-fold selectivity towards strand transfer inhibition. Compound **9**, complexed with boron, inhibited 3'-processing and strand transfer with IC₅₀ values of 9 and 3 μM, respectively.

Compounds **11** and **12** containing 3-acetyl-4-hydroxy-6-methyl-pyranone structure with a bulky, hydrophobic 1,3,3-trimethyl-2-methyleneindoline substitution were both inactive. Compounds **13** and **14** with a butylene bridge and *N,N*-dimethylaniline substitution did not show any IN inhibition, however compound **13** in the boron complex showed weak strand transfer inhibition with an IC₅₀ value of 100 μM. Compounds **15** and **16**, having a similar structure with the exception of a methoxy substitution, exhibited potent and selective strand transfer inhibition. As observed with the previous compounds, the boron complexed form of compound **15** has low IC₅₀ values, 11 and 4 μM for 3'-processing and strand transfer inhibition, respectively than the corresponding uncomplexed form. Further substitutions at the 6-methyl position resulted in compounds **17–22**. These compounds lacked any IN inhibitory activity.

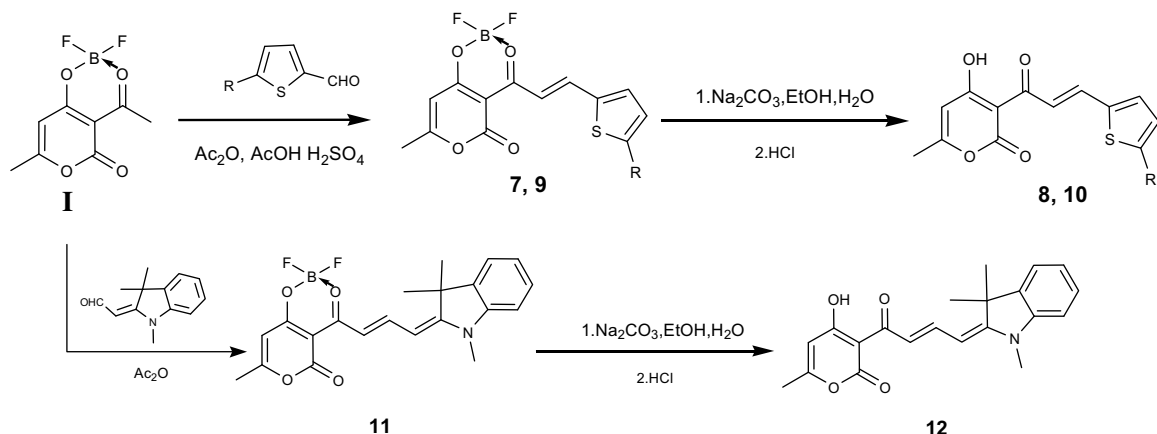
Overall, 3-acetyl-4-hydroxy-6-methyl-pyranones with hydrophobic substitutions separated by alkene bridges selectively inhibited IN strand transfer. Due to the shallow substrate binding site on IN, the size and position of the substituent in these compounds appear to play a critical role in determining IN inhibitory activities. Interestingly, complexation with boron difluoride increased the potency and selectivity of IN inhibition. Figure 1 shows the inhibition of IN catalytic activities by active compounds. Compound **9** stands out as the most potent compound in the set with an IC₅₀ va-



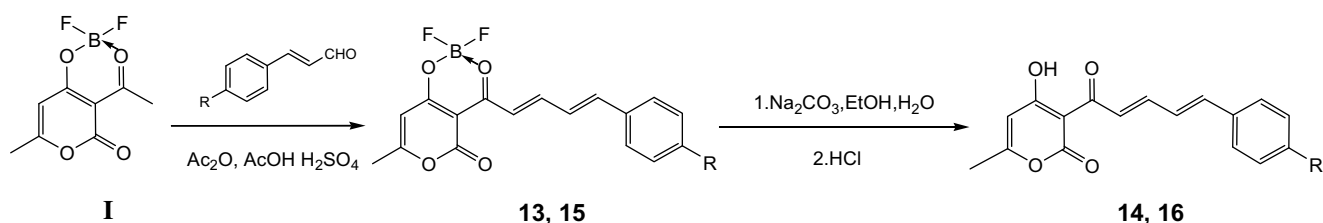
Scheme 1. Synthesis of compound **1**.



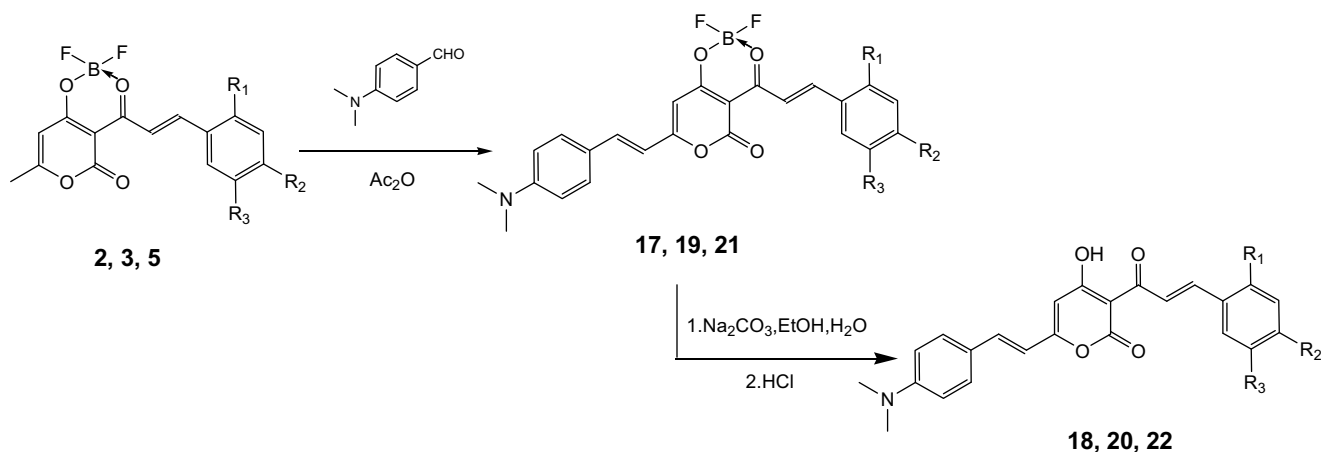
Scheme 2. Synthesis of compounds **2–6**. R = N(CH₃)₂ (**2**); R = Br (**3,4**); R = F (**5,6**).



Scheme 3. Synthesis of compounds **7–12**. R = N(CH₃)₂ (**7,8**); R = Br (**9, 10**).



Scheme 4. Synthesis of compounds **13–16**. R = N(CH₃)₂ (**13,14**); R = OCH₃ (**15,16**).



Scheme 5. Synthesis of compounds **17–22**. R₁ = R₃ = H, R₂ = N(CH₃)₂ (**17,18**); R₁ = R₃ = H, R₂ = OCH₃ (**19, 20**), R₁ = OCH₃, R₂ = H, R₃ = Br (**21, 22**).

lue of 9 μM for 3'-processing and 3 μM for strand transfer inhibition. These results were further studied and confirmed through molecular docking studies.

2.3. Cytotoxicity and antiviral studies

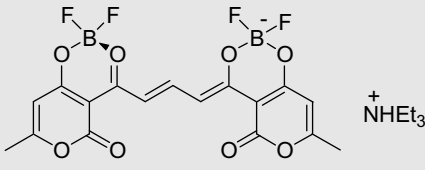
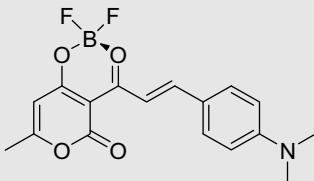
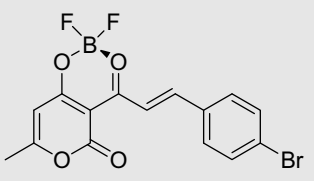
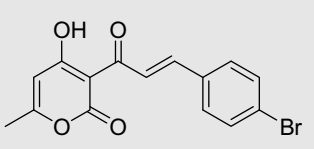
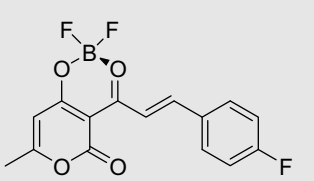
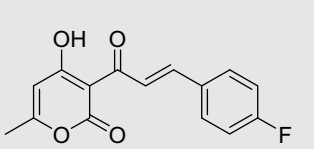
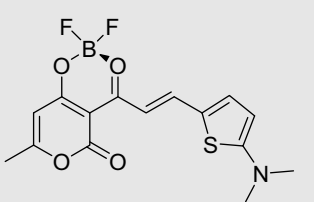
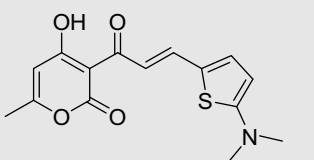
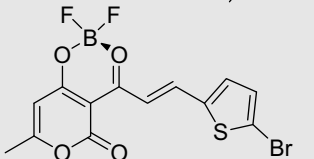
Cytotoxicity was assessed by cell viability in MTT assay. At 10 μM , none of the compounds exhibited any significant cytotoxicity. Compounds **1, 3, 9** and **15** with potent in vitro IN inhibitory effects showed no substantial antiviral activity. Further studies are in progress to design more potent analogs with improved antiviral activity.

2.4. Computational studies

Compounds **1–22** were docked onto IN active site using eHITS and GOLD in order to identify their binding sites. The GOLD fitness

scores and eHITS scores, along with selected physicochemical properties, are given in Table 2. A general trend was observed, in which the more active difluoroborate complexes scored higher than corresponding uncomplexed pyranones. Overall, there was no significant correlation between the fitness scores and IN inhibitory activities of the compounds. Figure 2 depicts a comparison between the bound conformation of representative active compound **3** inside the active site of IN and its corresponding inactive uncomplexed pyranone **4**. The predicted binding areas of **3** and **4** in the IN active site were similar to that of 5CITEP. Hydrogen bonding interactions and the interacting amino acid residues at the active site are given in Table 3. These compounds commonly occupy a wide cavity surrounded by the following amino acids: K159, K156, N155, E152, I151, P142, I141, G140, F139, N117, D116, H114, D64 and Q62. It was observed that the active compound **3** established strong interactions with key amino acid residues D64

Table 1
Inhibition of HIV-1 IN catalytic activities and cytotoxicity by substituted and boron complexed pyranones

Compound	Structure	Inhibition of IN catalytic activity IC ₅₀ (μM)			Cytotoxicity (μM) ^c
		3'-Processing ^a	Strand transfer ^a	Selectivity index ^b	
1		13 ± 8	7 ± 2	1.9	>10
2		>100	56 ± 1	>1.8	>10
3		12 ± 6	4 ± 2	3.3	>10
4		>100	>100	—	>10
5		9 ± 3	16 ± 4	0.6	>10
6		64	>100	<0.7	>10
7		>100	>100	—	>10
8		19 ± 4	11 ± 6	1.8	>10
9		9 ± 2	3 ± 2	3.2	> 10

(continued on next page)

Table 1 (continued)

Compound	Structure	Inhibition of IN catalytic activity IC ₅₀ (μM)			Cytotoxicity (μM) ^c
		3'-Processing ^a	Strand transfer ^a	Selectivity index ^b	
10		65 ± 40	23 ± 3	2.8	>10
11		>100	>100	—	>10
12		>100	>100	—	>10
13		>100	100	—	>10
14		>100	>100	—	>10
15		11 ± 3	4 ± 3	2.5	>10
16		>100	39 ± 14	>2.6	>10
17		>100	>100	—	>10
18		>100	>100	—	>10

Table 1 (continued)

Compound	Structure	Inhibition of IN catalytic activity IC ₅₀ (μM)			Cytotoxicity (μM) ^c
		3'-Processing ^a	Strand transfer ^a	Selectivity index ^b	
19		>100	>100	—	>10
20		>100	>100	—	>10
21		>100	>100	—	>10
22		>100	100	—	>10

^a Results are from at least three independent experiments.

^b Selectivity index = (IC₅₀(3'-processing)/IC₅₀(strand transfer)).

^c Determined by MTT assay.

and E152 and Mg²⁺ ion that are important for IN catalytic activity. The inactive compound **4** did not form such interactions in the active site of IN.

3. Conclusion

We have identified a novel class of IN inhibitors with a unique 3-acetyl-4-hydroxy-pyranone scaffold. Some of the difluoroborate complexes of the pyranones were found to be more potent IN inhibitors than uncomplexed pyranones. The potent and selective inhibition profile and the lack of cytotoxicity of these novel compounds make them suitable leads for further modifications. Structural optimization and mechanistic studies to enhance selective IN inhibitory activity is in progress.

4. Experimental

4.1. Chemistry

Compounds **1–22** were synthesized as a continuation of our previous studies on the synthesis, structure and reactivity of α,β -unsaturated ketones-3-acyl-4-hydroxycoumarin 3-acyl-4-hydroxy-2-quinolone derivatives and their analogs.^{19–21} ¹H NMR spectra was recorded on a Bruker WP-200-SY instrument in CDCl₃ and DMSO-*d*₆ with Me₄Si as the internal standard. The mass spectra were obtained on a MAT-112 mass spectrometer; the ionizing electron energy was 80 eV, the ion source temperature was equal to 250 °C, and the inlet temperature 240 °C.

4.1.1. 3-Acetyl-6-methyl-2-oxo-2H-pyran-4-yl difluoridoborate (**1**)

A solution of 3-acetyl-4-hydroxy-6-methyl-2-pyranone (10 g, 0.06 mol) in dry benzene (17 mL) was treated with boron trifluoride etherate (10 g, 0.07 mol) and heated for 1 h. The resultant precipitate was filtered, washed with benzene and crystallized from benzene. Complex **1**, yellow crystals, yield 80%, mp 156–157 °C. ¹H NMR (DMSO-*d*₆) δ , ppm: 2.39 (s, 3H, 6-CH₃), 2.86 (s, 3H, 3-CH₃), 6.13 (s, 1H, H⁵). Found %: C 44.45; H 3.21. C₈H₇BF₂O₄. Calculated %: C 44.50; H 3.27.

4.1.2. Triethylammonium 2,2-difluoro-4-[(O^{4'}-B)-4'-[(difluoroboryl)oxy]-4'-(4''-oxo-3'',4''-dihydropyranone-3''-ylidene)-2'-buten-1'-ylidene]di-oxaboratabenzo[c]pyranone (**1**)

A solution of a 3-acetyl-6-methyl-2-oxo-2H-pyran-4-yl difluoridoborate **1** (2 mmol) in acetic anhydride (5 mL) was treated with triethyl orthoformate (0.15 g, 1 mmol) and triethylamine (0.28 g, 2 mmol). The mixture was heated to 60 °C for 30 min and then cooled and allowed to stand for 4 h. The resultant precipitate was filtered, washed with hexane, and crystallized from glacial acetic acid. Compound **1**, yield 60%, mp 214–215 °C. ¹H NMR (DMSO-*d*₆) δ , ppm: 1.14 (t, 9H, 3CH₃), 2.23 (s, 6H, CH₃), 3.15 (q, 6H, 3CH₂), 6.16 (s, 2H, H⁵), 7.43 (d, 2H, CH), 8.87 (t, 1H, CH). MS, *m/z*: 441 [M⁺]. Found %: C 50.79; H 5.06; N 2.58. C₂₃H₂₇B₂F₄NO₈. Calculated %: C 50.87; H 5.01; N 2.58.

4.1.3. General procedure for the preparation of **2**, **7**, **11** and **13**

A solution of appropriate aldehyde (0.002 mol) in acetic anhydride (2 mL) was added to a solution of 3-acetyl-6-methyl-2-oxo-

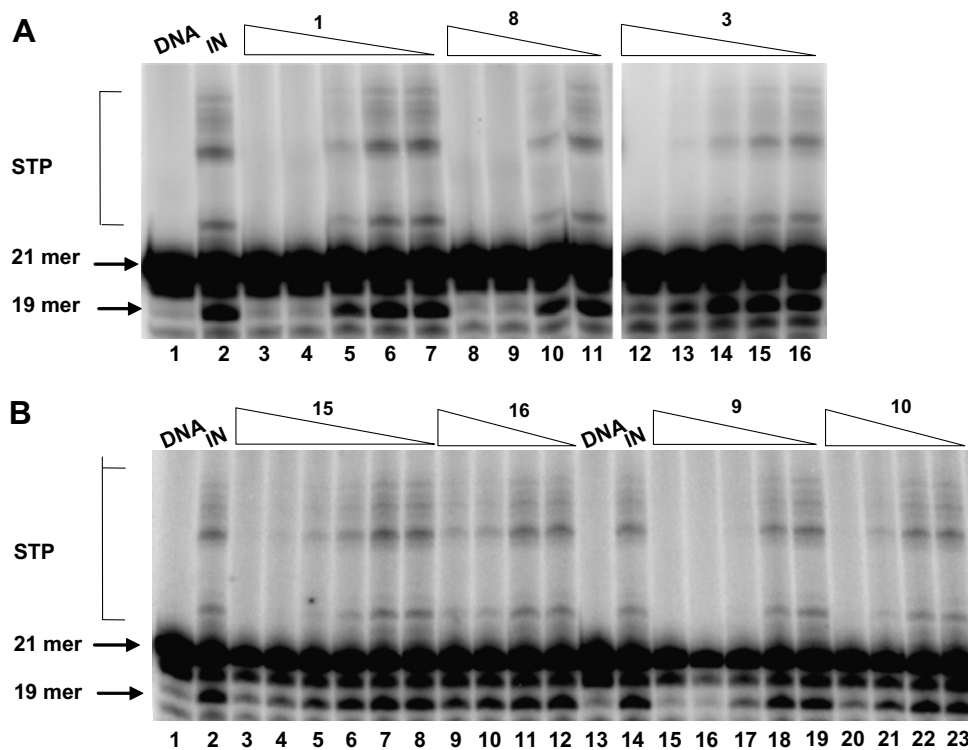


Figure 1. A representative gel showing inhibition of purified IN by selected compounds. (A) Lane 1—DNA alone; Lane 2—DNA and IN alone with no drug; Lanes 3–16—DNA with IN and selected drug concentrations (Compounds **1** and **3**—100, 33.3, 11.1, 3.7 and 1.2 μM ; Compound **8**—100, 33.3, 11.1 and 3.7 μM). (B) Lanes 1 and 13—DNA alone; Lanes 2 and 14—DNA and IN without drug; Lanes 3–12, 15–23—DNA with IN and selected drug concentrations (Compound **15**—100, 33.3, 11.1, 3.7, 1.2 and 0.4 μM ; Compound **9**—100, 33.3, 11.1, 3.7 and 1.2 μM ; Compounds **16** and **10**—100, 33.3, 11.1 and 3.7 μM).

Table 2
Docking scores and selected physicochemical properties of substituted and boron complexed pyranone

Compound	MW ^a	RB ^b	HBA ^c	HBD ^d	ALogP ^e	S + logP ^f	PSA ^g	eHits_Score	GOLD_Score
1	441.89	2	8	0	4.358	2.53	91.59	-1.08	51.99
2	347.12	3	5	0	3.82	3.80	50.07	-0.28	46.91
3	382.95	2	4	0	4.41	4.11	46.83	-2.59	49.89
4	335.15	3	4	1	2.87	3.88	63.60	-1.96	42.13
5	322.04	2	4	0	3.86	3.60	46.83	-1.68	46.55
6	274.24	3	4	1	2.33	3.35	63.60	-1.74	44.45
7	353.15	3	5	0	3.90	3.42	78.30	-2.15	42.36
8	305.35	4	5	1	2.36	2.92	95.08	-2.01	47.72
9	388.98	2	4	0	4.18	3.84	75.06	-1.38	50.76
10	341.18	3	4	1	2.64	3.53	91.84	-2.12	48.39
11	399.20	2	5	0	4.65	5.29	50.07	-2.41	42.10
12	351.40	3	5	1	3.12	4.61	66.84	-1.87	43.37
13	373.16	4	5	0	4.29	4.59	50.07	-1.62	43.43
14	325.36	5	5	1	2.75	3.85	66.84	-1.68	39.44
15	360.12	4	5	0	4.11	4.33	56.06	-1.75	54.98
16	312.32	5	5	1	2.57	3.65	72.83	-1.79	50.12
17	478.30	6	6	0	5.69	6.33	53.31	-0.62	42.35
18	430.50	7	6	1	4.15	5.48	70.08	-0.04	43.74
19	465.25	6	6	0	5.51	6.12	59.30	-1.10	48.97
20	417.45	7	6	1	3.97	5.36	76.06	-1.47	43.74
21	544.15	6	6	0	6.26	6.92	59.30	-0.67	41.48
22	496.35	7	6	1	4.72	6.15	76.07	-1.92	49.18

^a Molecular weight.

^b Number of rotatable bonds.

^c Number of H-bond acceptors.

^d Number of H-bond donors.

^e Calculated atom-based log P.

^f S + logP (Simulations Plus LogP model).

2H-pyran-4-yl difluoridoborate (0.5 g, 0.002 mol) in acetic anhydride (6 mL) at 60 °C. The mixture was then heated at 90 °C for 0.5 h. The reaction mixture was cooled; the precipitate formed was filtered and washed with acetic acid, and recrystallized from glacial acetic acid.

4.1.3.1. 3-((2E)-3-[4-(Dimethylamino)phenyl]prop-2-enoyl)-6-methyl-2-oxo-2H-pyran-4-yl difluoridoborate (2). Yield 84%, mp 238–239 °C. ¹H NMR (CDCl₃) δ , ppm: 2.34 (s, 3H, CH₃), 3.17 (s, 6H, N(CH₃)₂), 6.07 (s, 1H, H⁵), 6.70 (d, 2H, H^{ar}, J = 8.8 Hz), 7.68 (d, 2H, H^{ar}, J = 8.8 Hz), 8.08 (d, 1H, CH, J = 14.9 Hz), 8.42 (d, 1H,

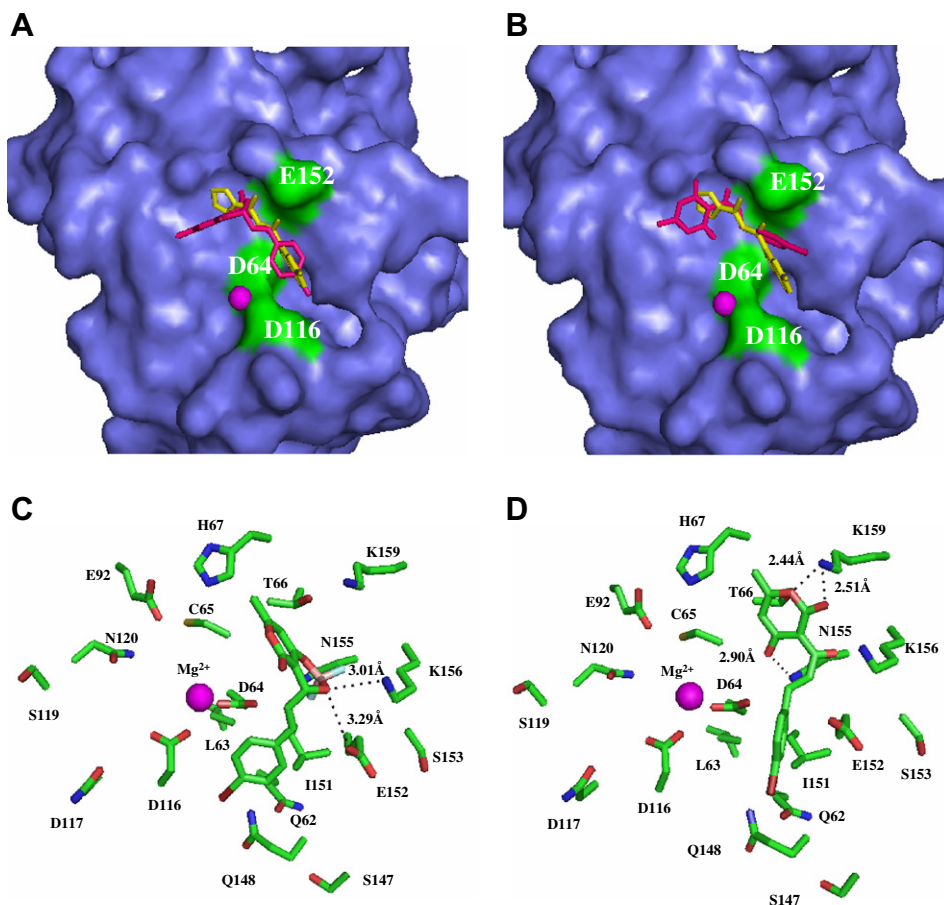


Figure 2. The bound conformation of compounds **3** and **4** on the catalytic core domain of HIV-1 IN. (A) and (B) shows the compounds **3** and **4** (pink), respectively overlaid on crystal ligand 5CITEP (yellow) and binding surface is shown in green. The magenta sphere represents metal ion (Mg^{2+}). (C) and (D) demonstrate the detailed interactions between IN and the ligands **3** and **4**, respectively.

Table 3

H-bonding interactions and the active site amino acid residues interacting with compounds **3** and **4**

Compound	H-bonding interactions ^a	Interacting amino acid residues
3	C=O...HO E152 (3.29) C=O HN K156 (3.01)	L63, D64, C65, T66, H67, E92, D116, Q148, I151, E152, N155, K156, K159
4	C=O HN N155 (2.51) C–O HN K159 (2.44)	D64, C65, T66, H67, D116, Q148, I151, E152, N155, K156, K159

^a Values in parentheses are H-bond distances in Å.

CH, $J = 14.9$ Hz). MS, m/z : 348 [M^+]. Found %: C 58.79; H 4.60; N 4.00. $C_{17}H_{16}BF_2NO_4$. Calculated %: C 58.82; H 4.65; N 4.04.

4.1.3.2. 3-((2E)-3-[5-(Dimethylamino)-2-thienyl]prop-2-enoyl]-6-methyl-2-oxo-2H-pyran-4-yl difluoridoborate (7). Yield 88%, mp 223–224 °C. 1H NMR (DMSO- d_6) δ , ppm: 2.26 (s, 3H, CH_3), 3.38 (s, 6H, $N(CH_3)_2$), 6.22 (s, 1H, H^5), 6.86 (d, 1H, H^{het} , $J = 5.1$ Hz), 7.06 (d, 1H, CH, $J = 12.9$ Hz), 8.01 (d, 1H, H^{het} , $J = 5.1$ Hz), 8.21 (d, 1H, CH, $J = 12.9$ Hz). MS, m/z : 354 [M^+]. Found %: C 51.04; H 4.09; N 3.96; S 9.10. $C_{15}H_{14}BF_2NO_4S$. Calculated %: C 51.02; H 4.00; N 3.97; S 9.08.

4.1.3.3. 6-Methyl-2-oxo-3-[(2E,4E)-4-(1,3,3-trimethyl-1,3-dihydro-2H-indol-2-ylidene)but-2-enoyl]-2H-pyran-4-yl difluoridoborate (11). Yield 76%, mp 250–251 °C. 1H NMR ($CDCl_3$) δ , ppm: 1.68 (s, 6H, $(CH_3)_2$), 2.29 (s, 3H, CH_3), 3.54 (s, 3H, $N(CH_3)_2$),

6.01 (s, 1H, H^5), 6.10 (d, 1H, CH, $J = 14$ Hz), 7.04–7.47 (m, 5H, $4H^{ar}$, CH), 8.73 (t, 1H, CH). MS, m/z : 400 [M^+]. Found %: C 63.15; H 5.10; N 3.49. $C_{21}H_{20}BF_2NO_4$. Calculated %: C 63.18; H 5.05; N 3.51.

4.1.3.4. 3-[(2E,4E)-5-[4-(Dimethylamino)phenyl]penta-2,4-dienoyl]-6-methyl-2-oxo-2H-pyran-4-yl difluoridoborate (13). Yield 64%, mp 242–243 °C. 1H NMR (DMSO- d_6) δ , ppm: 2.33 (s, 3H, CH_3), 3.31 (s, 6H, $N(CH_3)_2$), 6.41 (s, 1H, H^5), 6.79 (d, 2H, H^{ar} , $J = 8.7$ Hz), 7.28 (t, 1H, CH), 7.57 (d, 1H, CH, $J = 14.3$ Hz), 7.65 (d, 2H, H^{ar} , $J = 8.7$ Hz), 7.68 (d, 1H, CH, $J = 14.3$ Hz), 8.17 (t, 1H, CH). MS, m/z : 374 [M^+]. Found %: C 61.19; H 4.89; N 3.65. $C_{19}H_{18}BF_2NO_4$. Calculated %: C 61.16; H 4.86; N 3.75.

4.1.4. General procedure for the preparation of **3**, **5**, **9** and **15**

A solution of appropriate aldehyde (0.002 mol) in glacial acetic acid (2 mL) and sulfuric acid (0.13 mL) was added to a solution of 3-acetyl-6-methyl-2-oxo-2H-pyran-4-yl difluoridoborate (0.5 g, 0.002 mol) in glacial acetic acid (6 mL) at 60 °C. The mixture was then refluxed for 0.5 h. The reaction mixture was cooled; the precipitate that formed was filtered, washed with acetic acid, and recrystallized from glacial acetic acid.

4.1.4.1. 3-[(2E)-3-(4-Bromophenyl)prop-2-enoyl]-6-methyl-2-oxo-2H-pyran-4-yl difluoridoborate (3). Yield 80%, mp 195–196 °C. 1H NMR ($CDCl_3$) δ , ppm: 2.38 (s, 3H, CH_3), 6.16 (s, 1H, H^5), 7.62 (s, 4H, H^{ar}), 8.36 (s, 2H, CH). MS, m/z : 383 [M^+]. Found %: C 47.08; H 2.66. $C_{15}H_{10}BBF_2O_4$. Calculated %: C 47.05; H 2.63.

4.1.4.2. 3-[(2E)-3-(4-Fluorophenyl)prop-2-enoyl]-6-methyl-2-oxo-2H-pyran-4-yl difluoridoborate (5). Yield 65%, mp 176–177 °C. ¹H NMR (CDCl₃) δ, ppm: 2.40 (s, 3H, CH₃), 6.16 (s, 1H, H⁵), 7.76 (s, 4H, H^{ar}), 8.37 (s, 2H, CH). MS, *m/z*: 323 [M⁺]. Found %: C 55.96; H 3.18. C₁₅H₁₀BF₃O₄. Calculated %: C 55.94; H 3.13.

4.1.4.3. 3-[(2E)-3-(5-Bromo-2-thienyl)prop-2-enoyl]-6-methyl-2-oxo-2H-pyran-4-yl difluoridoborate (9). Yield 88%, mp 156–157 °C. ¹H NMR (CDCl₃) δ, ppm: 2.40 (s, 3H, CH₃), 6.13 (s, 1H, H⁵), 7.19 (d, 1H, H^{het}, *J* = 5.1 Hz), 7.38 (d, 1H, H^{het}, *J* = 5.1 Hz), 8.00 (d, 1H, CH, *J* = 12.9 Hz), 8.36 (d, 1H, CH, *J* = 12.9 Hz). MS, *m/z*: 389 [M⁺]. Found %: C 40.15; H 2.10; S 8.27. C₁₃H₈BBBrF₂O₄S. Calculated %: C 40.14; H 2.07; S 8.24.

4.1.4.4. 3-[(2E,4E)-5-(4-Methoxyphenyl)penta-2,4-dienoyl]-6-methyl-2-oxo-2H-pyran-4-yl difluoridoborate (15). Yield 74%, mp 198–199 °C. ¹H NMR (CDCl₃) δ, ppm: 2.36 (s, 3H, CH₃), 3.87 (s, 3H, OCH₃), 6.11 (s, 1H, H⁵), 6.92 (d, 2H, H^{ar}, *J* = 8.7 Hz), 7.02 (t, 1H, CH), 7.20 (d, 1H, CH, *J* = 14.3 Hz), 7.53 (d, 2H, H^{ar}, *J* = 8.7 Hz), 7.80 (d, 1H, CH, *J* = 14.3 Hz), 8.19 (t, 1H, CH). MS, *m/z*: 361 [M⁺]. Found %: C 60.08; H 4.16. C₁₈H₁₅BF₂O₅. Calculated %: C 60.03; H 4.20.

4.1.5. General procedure for the preparation of 17, 19 and 21

A solution of 4-dimethylaminobenzaldehyde (0.05 g, 0.4 mmol) in acetic anhydride (2 mL) was added to a solution of appropriate difluoridoborate (0.4 mmol) in acetic anhydride (2 mL) at 60 °C. The mixture was refluxed for 0.5 h. The reaction mixture was cooled; the precipitate that formed was filtered, washed with acetic acid, and recrystallized from glacial acetic acid.

4.1.5.1. 3-[(2E)-3-[4-(Dimethylamino)phenyl]prop-2-enoyl]-6-[(E)-2-[4-(dimethylamino)phenyl]vinyl]-2-oxo-2H-pyran-4-yl difluoridoborate (17). Yield 47%, mp 330–331 °C. ¹H NMR (DMSO-*d*₆+TFA) δ, ppm: 3.03 (s, 6H, N(CH₃)₂), 3.12 (s, 6H, N(CH₃)₂), 6.37 (s, 1H, H⁵), 6.82 (m, 4H, H^{ar}, *J* = 15.8 Hz), 7.60 (m, 3H, CH, H^{ar}), 7.71 (d, 2H, H^{ar}, *J* = 8.7 Hz), 7.86 (d, 1H, CH, *J* = 15.8 Hz), 8.00 (d, 1H, CH, *J* = 16.2 Hz), 8.15 (d, 1H, CH, *J* = 16.2 Hz). MS, *m/z*: 479 [M⁺]. Found %: C 65.24; H 5.23; N 5.86. C₂₆H₂₅BF₂N₂O₄. Calculated %: C 65.29; H 5.27; N 5.86.

4.1.5.2. 6-[(E)-2-[4-(Dimethylamino)phenyl]vinyl]-3-[(2E)-3-(4-methoxyphenyl)prop-2-enoyl]-2-oxo-2H-pyran-4-yl difluoridoborate (19). Yield 42%, mp 295–296 °C. ¹H NMR (DMSO-*d*₆+TFA) δ, ppm: 3.42 (s, 6H, N(CH₃)₂), 3.83 (s, 3H, OCH₃), 6.44 (s, 1H, H⁵), 6.74 (d, 2H, H^{ar}, *J* = 8.6 Hz), 6.84 (d, 1H, CH, *J* = 15.7 Hz), 7.08 (d, 2H, H^{ar}, *J* = 8.7 Hz), 7.60 (d, 2H, H^{ar}, *J* = 8.6 Hz), 7.74 (d, 1H, CH, *J* = 15.7 Hz), 7.81 (d, 2H, H^{ar}, *J* = 8.7 Hz), 8.17 (d, 1H, CH, *J* = 16 Hz), 8.28 (d, 1H, CH, *J* = 16 Hz). MS, *m/z*: 466 [M⁺]. Found %: C 64.50; H 4.73; N 3.01. C₂₅H₂₂BF₂NO₅. Calculated %: C 64.54; H 4.77; N 3.01.

4.1.5.3. 3-[(2E)-3-(5-Bromo-2-methoxyphenyl)prop-2-enoyl]-6-[(E)-2-[4-(dimethylamino)phenyl]vinyl]-2-oxo-2H-pyran-4-yl difluoridoborate (21). Yield 38%, mp 345–346 °C. ¹H NMR (DMSO-*d*₆+TFA) δ, ppm: 3.08 (s, 6H, N(CH₃)₂), 3.96 (s, 3H, OCH₃), 6.37 (s, 1H, H⁵), 6.71–6.85 (m, 3H, CH, H^{ar}), 7.10 (d, 1H, H^{ar}, *J* = 7.8 Hz), 7.53 (d, 1H, H^{ar}, *J* = 7.8 Hz), 7.63 (m, 3H, H^{ar}, CH), 7.73 (s, 1H, H^{ar}), 8.02 (d, 1H, CH, *J* = 15.8 Hz), 8.23 (d, 1H, CH, *J* = 15.8 Hz). MS, *m/z*: 546 [M⁺]. Found %: C 55.21; H 3.92; N 2.58. C₂₅H₂₁BBBrF₂NO₅. Calculated %: C 55.18; H 3.89; N 2.57.

4.1.6. General procedure for the preparation of 4, 6, 8, 10, 12, 14, 16, 18, 20 and 22

Appropriate difluoridoborate was dissolved in (10 mL) aqueous alcoholic solution of sodium carbonate (1.60 g, 15 mmol). The mixture was refluxed for 1–5 h. The reaction mixture was cooled, fil-

tered, treated with a solution of hydrochloric acid (pH 6.5–7). The precipitate that formed was filtered, washed with water, and recrystallized in isopropanol.

4.1.6.1. 3-[(2E)-3-(4-Bromophenyl)prop-2-enoyl]-4-hydroxy-6-methyl-2H-pyran-2-one (4). Yield 63%, mp 128–129 °C. ¹H NMR (CDCl₃) δ, ppm: 2.28 (s, 3H, CH₃), 5.96 (s, 1H, H⁵), 7.25 (s, 4H, Har), 7.83 (d, 1H, CH, *J* = 15.9 Hz), 8.25 (d, 1H, CH, *J* = 15.9 Hz), 17.75 (s, 1H, OH). MS, *m/z*: 336 [M⁺]. Found %: C 53.77; H 3.35. C₁₅H₁₁BrO₄. Calculated %: C 53.76; H 3.31.

4.1.6.2. 3-[(2E)-3-(4-Fluorophenyl)prop-2-enoyl]-4-hydroxy-6-methyl-2H-pyran-2-one (6). Yield 55%, mp 114–115 °C. ¹H NMR (CDCl₃) δ, ppm: 2.27 (s, 3H, CH₃), 5.95 (s, 1H, H⁵), 7.26 (s, 4H, Har), 7.95 (d, 1H, CH, *J* = 15.9 Hz), 8.28 (d, 1H, CH, *J* = 15.9 Hz), 17.84 (s, 1H, OH). MS, *m/z*: 275 [M⁺]. Found %: C 65.73; H 4.05. C₁₅H₁₁FO₄. Calculated %: C 65.69; H 4.04.

4.1.6.3. 3-[(2E)-3-[5-(Dimethylamino)-2-thienyl]prop-2-enoyl]-4-hydroxy-6-methyl-2H-pyran-2-one (8). Yield 88%, mp 190–191 °C. ¹H NMR (DMSO-*d*₆) δ, ppm: 2.17 (s, 3H, CH₃), 3.16 (s, 6H, N(CH₃)₂), 6.04 (s, 1H, H⁵), 6.25 (d, 1H, H^{het}, *J* = 4.1 Hz), 7.26 (d, 1H, CH, *J* = 14.3 Hz), 7.57 (d, 1H, H^{het}, *J* = 4.1 Hz), 8.04 (d, 1H, CH, *J* = 14.3 Hz), 14.00 (s, 1H, OH). MS, *m/z*: 306 [M⁺]. Found %: C 59.03; H 4.98; N 4.63; S 10.56. C₁₅H₁₅NO₄S. Calculated %: C 59.00; H 4.95; N 4.59; S 10.50.

4.1.6.4. 3-[(2E)-3-(5-Bromo-2-thienyl)prop-2-enoyl]-4-hydroxy-6-methyl-2H-pyran-2-one (10). Yield 76%, mp 115–116 °C. ¹H NMR (CDCl₃) δ, ppm: 2.27 (s, 3H, CH₃), 5.94 (s, 1H, H⁵), 7.05 (d, 1H, H^{het}, *J* = 4.1 Hz), 7.16 (d, 1H, H^{het}, *J* = 4.1 Hz), 7.87 (d, 1H, CH, *J* = 14.3 Hz), 7.98 (d, 1H, CH, *J* = 14.3 Hz), 17.80 (s, 1H, OH). MS, *m/z*: 342 [M⁺]. Found %: C 45.81; H 2.69; S 9.42. C₁₃H₉BrO₄S. Calculated %: C 45.77; H 2.66; S 9.40.

4.1.6.5. 4-Hydroxy-6-methyl-3-[(2E,4E)-4-(1,3,3-trimethyl-1,3-dihydro-2H-indol-2-ylidene)but-2-enoyl]-2H-pyran-2-one (12). Yield 76%, mp 250–251 °C. ¹H NMR (CDCl₃) δ, ppm: 1.66 (s, 6H, (CH₃)₂), 2.20 (s, 3H, CH₃), 3.32 (s, 3H, N(CH₃)₂), 5.85 (s, 1H, H⁵), 6.17 (d, 1H, CH, *J* = 14 Hz), 6.78–7.48 (m, 5H, 4H^{ar} CH), 8.39 (t, 1H, CH), 18.82 (s, 1H, OH). MS, *m/z*: 352 [M⁺]. Found %: C 71.75; H 6.08; N 4.02. C₂₁H₂₁NO₄. Calculated %: C 71.78; H 6.02; N 3.99.

4.1.6.6. 3-[(2E,4E)-5-[4-(Dimethylamino)phenyl]penta-2,4-dienoyl]-4-hydroxy-6-methyl-2H-pyran-2-one (14). Yield 72%, mp 204–205 °C. ¹H NMR (DMSO-*d*₆) δ, ppm: 2.23 (s, 3H, CH₃), 2.30 (s, 6H, N(CH₃)₂), 6.19 (s, 1H, H⁵), 6.72 (d, 2H, H^{ar}, *J* = 8.7 Hz), 7.07–7.71 (m, 6H, 2H^{ar}, 4CH). MS, *m/z*: 326 [M⁺]. Found %: C 70.10; H 5.92; N 4.31. C₁₉H₁₉NO₄. Calculated %: C 70.14; H 5.89; N 4.30.

4.1.6.7. 4-Hydroxy-3-[(2E,4E)-5-(4-methoxyphenyl)penta-2,4-dienoyl]-6-methyl-2H-pyran-2-one (16). Yield 74%, mp 156–157 °C. ¹H NMR (CDCl₃) δ, ppm: 2.28 (s, 3H, CH₃), 3.84 (s, 3H, OCH₃), 5.92 (s, 1H, H⁵), 6.88–7.79 (m, 8H, 4H^{ar}, 4CH), 18.18 (s, 1H, OH). MS, *m/z*: 313 [M⁺]. Found %: C 69.20; H 5.11. C₁₈H₁₆O₅. Calculated %: C 69.22; H 5.16.

4.1.6.8. 3-[(2E)-3-[4-(Dimethylamino)phenyl]prop-2-enoyl]-6-[(E)-2-[4-(dimethylamino)phenyl]vinyl]-4-hydroxy-2H-pyran-2-one (18). Yield 72%, mp 256–257 °C. ¹H NMR (DMSO-*d*₆+TFU) δ, ppm: 3.51 (s, 12H, 2N(CH₃)₂), 6.52 (s, 1H, H⁵), 6.92 (d, 1H, CH, *J* = 15.8 Hz), 7.67 (d, 2H, H^{ar}, *J* = 8.8 Hz), 7.71 (d, 2H, H^{ar}, *J* = 8.7 Hz), 7.75 (d, 1H, CH, *J* = 15.8 Hz), 7.87 (d, 2H, H^{ar}, *J* = 8.8 Hz), 7.99 (d, 2H, H^{ar}, *J* = 8.7 Hz), 8.03 (d, 1H, CH, *J* = 16.2 Hz), 8.44 (d, 1H, CH, *J* = 16.2 Hz). MS, *m/z*: 431 [M⁺]. Found %: C 72.50; H 6.01; N 6.50. C₂₆H₂₆N₂O₄. Calculated %: C 72.54; H 6.09; N 6.51.

4.1.6.9. 6-((E)-2-[4-(Dimethylamino)phenyl]vinyl)-4-hydroxy-3-[(2E)-3-(4-methoxyphenyl)prop-2-enoyl]-2H-pyran-2-one (20). Yield 64%, mp 240–241 °C. ¹H NMR (DMSO-*d*₆ + TFA) δ, ppm: 3.06 (s, 6H, N(CH₃)₂), 3.83 (s, 3H, OCH₃), 6.40 (s, 1H, H⁵), 6.87 (d, 1H, CH, *J* = 15.7 Hz), 7.67 (d, 2H, H^{ar}, *J* = 8.6 Hz), 7.64 (d, 2H, H^{ar}, *J* = 8.7 Hz), 7.78 (d, 1H, CH, *J* = 15.7 Hz), 7.84 (d, 2H, H^{ar}, *J* = 8.6 Hz), 7.95 (d, 2H, H^{ar}, *J* = 8.7 Hz), 8.13 (d, 1H, CH, *J* = 16 Hz), 8.24 (d, 1H, CH, *J* = 16 Hz). MS, *m/z*: 418 [M+]. Found %: C 71.85; H 5.59; N 3.32. C₂₅H₂₃NO₅. Calculated %: C 71.93; H 5.55; N 3.36.

4.1.6.10. 3-[(2E)-3-(5-Bromo-2-methoxyphenyl)prop-2-enoyl]-6-((E)-2-[4-(dimethylamino)phenyl]vinyl)-4-hydroxy-2H-pyran-2-one (22). Yield 65%, mp 263–264 °C. ¹H NMR (DMSO-*d*₆+TFA) δ, ppm: 3.05 (s, 6H, N(CH₃)₂), 3.87 (s, 3H, OCH₃), 6.32 (s, 1H, H⁵), 6.85 (d, 1H, CH, *J* = 16 Hz), 7.05 (m, 3H, H^{ar}), 7.55 (m, 2H, H^{ar}, CH), 7.65 (d, 2H, H^{ar}, *J* = 6.8 Hz), 7.74 (s, 1H, H^{ar}), 7.97 (d, 1H, CH, *J* = 16 Hz), 8.25 (d, 1H, CH, *J* = 16 Hz). MS, *m/z*: 497 [M+]. Found %: C 60.52; H 4.50; N 2.80. C₂₅H₂₂BrNO₅. Calculated %: C 60.50; H 4.47; N 2.82.

4.2. Biological activity

4.2.1. Materials, chemicals and enzymes

All compounds were dissolved in DMSO, and stock solutions were stored at –20 °C. γ-[³²P]-ATP was purchased either from Amersham Biosciences or ICN. The expression system for wild-type IN was a generous gift of Dr. Robert Craigie, Laboratory of Molecular Biology, NIDDK, NIH (Bethesda, MD).

4.2.2. Preparation of oligonucleotide substrates

21-mer oligonucleotides [21top (5'-GTGTGGAAAATCTCTAG CAGT-3') and 21bot (5'-ACTGCTAGAGATTTTCCA CAC-3')] were purchased from Norris Cancer Center Microsequencing Core Facility (University of Southern California) and purified by UV shadowing on polyacrylamide gel. To analyze the extent of 3'-processing and strand transfer with 5'-end labeled substrates, 21top was 5'-end labeled by using T4 polynucleotide kinase (Epicentre, Madison, WI) and [γ-³²P]-ATP (Amersham Biosciences or ICN). The kinase was heat-inactivated and 21bot was added in 1.5 M excess. The mixture was heated at 95 °C, allowed to slowly cool to room temperature, and purified through a spin 25 minicolumn (USA Scientific, Ocala, FL) to separate annealed double-stranded oligonucleotide from unincorporated material.

4.2.3. In vitro IN inhibition assay

To determine the extent of 3'-processing and strand transfer, wild-type IN was preincubated at a final concentration of 200 nM with the inhibitor in the reaction buffer [50 mM NaCl, 1 mM HEPES (pH 7.5), 50 μM EDTA, 50 μM dithiothreitol, 10% glycerol (w/v), 7.5 mM MnCl₂, 0.1 mg mL⁻¹ bovine serum albumin, 10 mM 2-mercaptoethanol, 10% dimethyl sulfoxide, and 25 mM MOPS (pH 7.2)] at 30 °C for 30 min. Next, 20 nM of the 5'-end ³²P-labeled linear oligonucleotide substrate was added, and incubation for an additional 1 h. Reactions were quenched by addition of 50× of loading dye (98% deionized formamide, 10 mM EDTA, 0.025% xylene cyanol, and 0.025% bromophenol blue). An aliquot (5 μL) was subjected to electrophoresis on a denaturing polyacrylamide gel (0.09 M Tris-borate, pH 8.3, 2 mM EDTA, 20% acrylamide, 8 M urea). Gels were dried under vacuum, exposed in a PhosphorImager cassette and visualized with a Typhoon 8610 Variable Mode Imager (Amersham Biosciences). Quantification was done with Image Quant 5.2 software. Percent inhibition (%I) was calculated using the following equation:

$$\%I = 100 \times [1 - (D - C)/(N - C)], \quad (1)$$

where C, N, and D are the fractions of 21-mer substrate converted into 19-mer (product of 3'-processing) or strand-transfer products for DNA alone, DNA plus IN without drug and with drug, respectively. IC₅₀ values were determined by plotting the logarithm of drug concentration as a function of %I to obtain the concentration that produced 50% inhibition.^{5,22}

4.2.4. Cytotoxicity assay

Human colon cancer cell line HCT-116 was maintained as a monolayer culture and 8 × 10³ cells were seeded into each well on a 96-well tissue culture plate. After overnight attachment, compounds dissolved in RPMI-1640 medium (with 10% bovine serum albumin) were added to a final concentration of 10 μM. After 72 h, 3-(4,5-dimethylthiazol-2-yl)-2,5-diphenyltetrazolium bromide (MTT) solution (5 mg/mL; 20 μL) was added into the cell culture plate and incubated with cells for 4 h. The media from each well was removed and the cell-associated MTT crystals were dissolved in DMSO (150 μL/well) on a shaker at room temperature. The absorbance intensity was measured at 570 nm against appropriate blank controls using a microplate reader from Molecular devices.²³

4.3. Computational studies

Compounds **1–22** were docked onto the active site of IN to determine the biologically active conformation and possible mechanism of binding with IN. Docking calculations were performed using GOLD²⁴ and eHITS²⁵ software packages on co-crystal structures of IN (described below).

4.3.1. Ligand preparation

The structures of compounds **1–22** were built and minimized using Catalyst (Accelrys, Inc.) running on a multiprocessor Linux machine and a 24-processor Silicon Graphics Onyx workstation. The poling algorithm implemented within Catalyst was used to generate conformations for each compound. All feasible unique conformations were generated over a 20 kcal/mol range of energies using the best flexible conformation generation method in Catalyst. The lowest energy conformation of each ligand was chosen for docking simulation.

4.3.2. Protein preparation

The crystal structure of IN with its bound inhibitor 5CITEP (1-(5-chloroindol-3-yl)-3-hydroxy-3-(2H-tetrazol-5-yl)-propanone) from the Protein Data Bank (PDB entry 1QS4)²⁶ was used for the docking simulations. Some residues were unresolved in each chain of the X-ray crystal structure. Chain A, which binds to 5-CITEP and also orients Mg²⁺ chelating residues D64 and D116, was selected as the docking target. The four unresolved residues from chain A were modeled. Y143 and N144 were obtained from chain B of 1QS4, while residues I141 and P142 were modeled from the IN structure 1BIS via backbone alignment. Entire modeling and minimization of protein was done using Insight II suite of software (Accelrys, Inc). All water molecules present in the crystal structure were removed, but Mg²⁺ ion was left unchanged. Hydrogen atoms were added, the acidic and basic residues in the active site were in their ionic form, and the protonation state of protein at pH 7.0 was retained during the docking studies. The ligand (5CITEP) was subsequently removed to make the binding pocket available during simulations studies.

4.3.3. GOLD v. 3.2

Docking studies of IN inhibitors were carried out using the GOLD software package running on our multi-processor linux machine and a 24-processor Silicon Graphics Onyx workstation. A collection of minimized compounds (**1–22**) were docked on to IN

active site with the GOLD. A spherical area with a radius of 20 Å was defined and centered at the carboxylate oxygen (OD1) of D64 in the active site. Standard set parameters of GOLD were used throughout the simulations. For each of the 10 independent genetic algorithm runs, with a selection pressure of 1.1, 100,000 operations were performed on a set of 5 islands with a population size of 100 individuals. Default operator weights were used for crossover, mutation, and migration of 95, 95 and 10, respectively. Default cut-offs values of 2.5 Å for hydrogen bonds and 4.0 Å for van der Waals were employed. All other values were set to the default. Top 20 poses were saved for each ligand and best score values were used to correlate with experimental data.

4.3.4. eHITS

Docking for these 22 compounds was also performed using eHITS docking program. All docking simulations using eHITS were performed on parallel nodes at Sun Grid Compute Utility accessed at <http://Network.com>. eHITS automatically evaluates all possible protonation states of the receptor and ligands for each receptor-ligand pair. The docking method systematically covers the conformational and positional search space to avoid severe steric clashes. The top 20 conformations were saved and eHITS scores were calculated for each of the 20 saved ligand conformations. The highest score of each ligand was selected to correlate with its biological activity.

4.3.5. Computational ADMET analysis

Structures of all compounds were exported to ADMET Predictor (Simulations Plus, Inc.) to calculate properties such as MW, number of rotatable bonds, number of hydrogen bond donors, number of hydrogen bond acceptor, and $S + \log P$. $A \log P$ 98 and polar surface area was calculated using Discovery studio (Accelrys, Inc.).

Acknowledgments

Work in Dr. Neamati's laboratory was supported by funds from The Campbell Foundation. Work at D. Mendeleev University of Chemical Technology was carried out as a part of the research project of the Russian Foundation of Basic Research, N 07-03-00936.

References and notes

- Brown, P. O. In *Retroviruses*; Coffin, J. M., Hughes, S. H., Varmus, H. E., Eds.; Cold Spring Harbor Laboratory Press: Cold Spring Harbor, Woodbury, NY, 1997; pp 161–203.
- Dayam, R.; Gundla, R.; Al-Mawsawi, L. Q.; Neamati, N. *Med. Res. Rev.* **2008**, *28*, 118.
- Nair, V.; Chi, G. *Rev. Med. Virol.* **2007**, *17*, 277.
- Neamati, N. *Expert Opin. Ther. Pat.* **2002**, *12*, 709.
- Dayam, R.; Sanchez, T.; Neamati, N. *J. Med. Chem.* **2005**, *48*, 8009.
- Deng, J.; Sanchez, T.; Al-Mawsawi, L. Q.; Dayam, R.; Yunes, R. A.; Garofalo, A.; Bolger, M. B.; Neamati, N. *Bioorg. Med. Chem.* **2007**, *15*, 4985.
- Carlson, H. A.; Masukawa, K. M.; Rubins, K.; Bushman, F. D.; Jorgensen, W. L.; Lins, R. D.; Briggs, J. M.; McCammon, J. A. *J. Med. Chem.* **2000**, *43*, 2100.
- Deng, J.; Lee, K. W.; Sanchez, T.; Cui, M.; Neamati, N.; Briggs, J. M. *J. Med. Chem.* **2005**, *48*, 1496.
- Pommier, Y.; Johnson, A. A.; Marchand, C. *Nat. Rev. Drug Discov.* **2004**, *4*, 236.
- Hazuda, D. J.; Young, S. D.; Guare, J. P.; Anthony, N. J.; Gomez, R. P.; Wai, J. S.; Vacca, J. P.; Handt, L.; Motzel, S. L.; Klein, H. J.; Dornadula, G.; Danovich, R. M.; Witmer, M. V.; Wilson, K. A. A.; Tussey, L.; Schleif, W. A.; Gabryelski, L. S.; Jin, L.; Miller, M. D.; Casimiro, D. R.; Emini, E. A.; Shiver, J. W. *Science* **2004**, *305*, 528.
- Cooper, D.; Gatell, J.; Rockstroh, J.; Katlama, C.; Yeni, P.; Lazzarin, A.; Chen, J.; Isaacs, R.; Teppler, H.; Nguyen, B. Y. *Abstract of papers*, 14th Conference on Retroviruses and Opportunistic Infections, Los Angeles, CA, February 25–28, **2007**; 105aLB.
- Dayam, R.; Al-Mawsawi, L. Q.; Neamati, N. *Drugs R&D* **2007**, *8*, 155.
- Sato, M.; Motomura, T.; Aramaki, H.; Matsuda, T.; Yamashita, M.; Ito, Y.; Kawakami, H.; Matsuzaki, Y.; Watanabe, W.; Yamataka, K.; Ikeda, S.; Kodama, E.; Matsuoka, M.; Shinkai, H. *J. Med. Chem.* **2006**, *49*, 1506.
- Lataillade, M.; Kozal, M. J. *AIDS Patient Care STDS* **2006**, *20*, 489.
- Bransová, J.; Brtko, J.; Uher, M.; Novotný, L. *Int. J. Biochem. Cell. Biol.* **1995**, *27*, 701.
- Gupta, S. P.; Babu, M. S.; Kaw, N. *J. Enzyme Inhib.* **1999**, *14*, 109.
- Barth, R. F.; Coderre, J. A.; Vicente, M. G.; Blue, T. E. *Clin. Cancer Res.* **2005**, *11*, 3987.
- Cigler, P.; Kozisek, M.; Rezacová, P.; Brynda, J.; Otwinowski, Z.; Pokorná, J.; Plešek, J.; Grüner, B.; Dolecková-Maresová, L.; Mása, M.; Sedláček, J.; Bodem, J.; Kräusslich, H. G.; Král, V.; Konvalinka, J. *Proc. Natl. Acad. Sci. U.S.A.* **2005**, *102*, 15394.
- Traven, V. F.; Manaev, A. V.; Chibisova, T. A. *Dyes Pigments* **2003**, *58*, 41.
- Manaev, A. V.; Chibisova, T. A.; Lyssenko, K. A.; Antipin, M. Yu.; Traven, V. F. *Russ. Chem. Bull.* **2006**, *55*, 2091.
- Manaev, A. V.; Chibisova, T. A.; Traven, V. F. *Russ. Chem. Bull.* **2006**, *55*, 2223.
- Al-Mawsawi, L. Q.; Fikkert, V.; Dayam, R.; Witvrouw, M.; Burke, T. R., Jr.; Borchers, C. H.; Neamati, N. *Proc. Natl. Acad. Sci. U.S.A.* **2006**, *103*, 10080.
- Burger, A. M.; Jenkins, T. C.; Double, J. A.; Bibby, M. C. *Br. J. Cancer* **1999**, *81*, 367.
- GOLD. 1.2; CCDC: Cambridge, UK, **2002**.
- Zsoldos, Z.; Reid, D.; Simon, A.; Sadjad, S. B.; Johnson, A. P. *J. Mol. Graph. Model.* **2007**, *26*, 198.
- Goldgur, Y.; Craigie, R.; Cohen, G. H.; Fujiwara, T.; Yoshinaga, T.; Fujishita, T.; Sugimoto, H.; Endo, T.; Murai, H.; Davies, D. R. *Proc. Natl. Acad. Sci. U.S.A.* **1999**, *96*, 13040.